

SITE-SPECIFIC RESPONSE ANALYSIS & DEVELOPMENT OF TIME SERIES FOR NEAR-FAULT SITES

Sindhu Rudianto

Principal – PT. Geo Prima

Masyhur Irsyam

Professor – Bandung Institute of Technology

Iswandi Imran

Professor – Bandung Institute of Technology

Tony Sihite

Director – PT. Delta Global Struktur

ABSTRAK: Infrastruktur seperti jembatan, bendungan dan bangunan sering kali direncanakan pada lokasi dekat sesar aktif ($M_w > 6$, $D < 10$ km), sehingga proyek bisa tergolong sebagai Situs Dekat Sesar (SDS). Makalah ini membahas kasus studi jembatan dekat dengan sesar Opak ($M6.9$, $D5.5$ km) dimana analisa struktur jembatan mengharuskan pemakaian tujuh pasang riwayat waktu (time series) dalam arah horizontal dan vertikal. Untuk lokasi dekat sesar, ada dua faktor yang harus diperhatikan yakni efek forward directivity yang bisa menyebabkan Pulse-dan-Fling-step. Efek dari forward directivity adalah terjadinya rambatan gelombang dalam arah fault normal (FN) yang lebih kuat dibandingkan dengan arah fault parallel (FP). Karenanya, desain spektrum respons juga dibedakan dalam arah fault normal (FN) dan fault parallel (FP). Makalah ini membahas pemilihan time series yang harus memperhatikan adanya “pulse-motion” dalam arah fault-normal (FN). Karenanya, dalam pemilihan tujuh pasang time series, harus ada empat pasang no-pulse motion yang mewakili sesar aktif dan gempa subduksi dan tiga pasang pulse motion yang mewakili sesar aktif dengan durasi pendek dimana Peak Ground Velocity (PGV) dan Pulse Period (T_p) lebih mengontrol daripada spektrum respons percepatan.

Kata Kunci: Directivity, pulse motion, fault normal

ABSTRACT: Infrastructure such as bridges, dams and buildings are often built at locations near active faults ($M_w > 6$, $D < 10$ km), such that the projects can be classified as Near-Fault Sites (NFS). This paper presents case history of designing a bridge near Opak fault ($M6.9$, $D5.5$ km) where the analysis of the bridge structure requires seven sets of earthquake time series in the horizontal and vertical directions. For locations at near-fault, it must consider the effect of forward directivity that may cause pulse and fling-step. The effect of forward directivity is the occurrence of wave propagation in the normal fault direction (FN) which is stronger than the direction of the fault parallel (FP). Accordingly, the design of the response spectrum is distinguished in the direction of normal fault (FN) and parallel fault (FP). This paper discusses the selection of seven sets time series, where four pairs of no-pulse motions representing active faults and subduction earthquakes and three pairs of pulse motions representing near-faults where Ground Velocity (PGV) and Pulse Period (T_p) are more controlling than the acceleration response spectrum.

Keywords: Directivity, pulse motion and fault normal

1 INTRODUCTION

Infrastructure development such as bridges, buildings, and dams are often built near shallow crustal faults, making Near Fault Site (NFS) very common when considering earthquake resistant facilities. According to SNI 2833-2016 (Indonesian Seismic Code for Bridge), Near-Faults Site is defined when the

facility is located at distance less than 10 km away from the projected active fault (defined as slip rate > 1 mm per year) with depth of less than 10 km and capable of producing earthquake events with $M_w > 6$.

Near-fault ground motions are significantly influenced by the rupture mechanism and slip direction relative to the site and by the permanent ground displacement at the site

resulting from tectonic movement. When the rupture and slip direction relative to a site coincide, and a significant portion of the fault ruptures towards the site, the ground motion can exhibit the effects of forward-directivity (FD). Most of the energy in FD motions is concentrated in a narrow frequency band and is expressed as one or more high intensity velocity pulses oriented in the fault-normal (FN) direction and cause pulse motion. These intense velocity pulses can lead to severe structural damage.

Ground motions close to the surface rupture may also contain a significant permanent displacement, which is called “fling-step”, and this may lead to a high intensity velocity pulse in the direction of the fault displacement. Pulses from fling-step have different characteristics than FD pulses. While FD is a dynamic phenomenon that produces no permanent ground displacement and consequently two-sided velocity pulses, fling-step is a result of a permanent ground displacement that generates one sided velocity pulses. The development of design ground motions for a project site close to an active fault should account for these special aspects of near-fault ground motions.

Research during the past decade showed that ground motion due to these “pulse motions” could result in significant damage to the structure. For instance, this is evident from experimental tests and observations of earthquakes in Northridge (1994) and Kobe (1995). The analytical models from Krawinkler and Alavi (2004) also show that traditional methods of analysis are not sufficient to capture the full effects of earthquake shocks due to this “pulse motion”. With a plethora of earthquake records, especially from shallow crustal faults, the characterization of near-fault ground motions that could cause “pulse motions” can be distinguished more definitively.

This paper discusses a case study, where bridge structure will be built at location about 5.5 km from the active Opak fault (slip rate of 2 mm per year) and capable of producing an earthquake of Mw6.9. Bridge design requires the use of “damper”, where it is necessary to develop seven sets time series in the horizontal and vertical directions for Non-Linear Time History Analyses (NLTHA).

2 PSHA VS. DSHA

According to the LAPI Geological report (2021), there are three shallow crustal faults at the project vicinity (Fig. 1) that must be considered in calculating the Deterministic Seismic Hazard Analyses (DSHA). These faults are Opak Utama, Opak 1, and Mataram Timur faults with information is listed on Table 1.

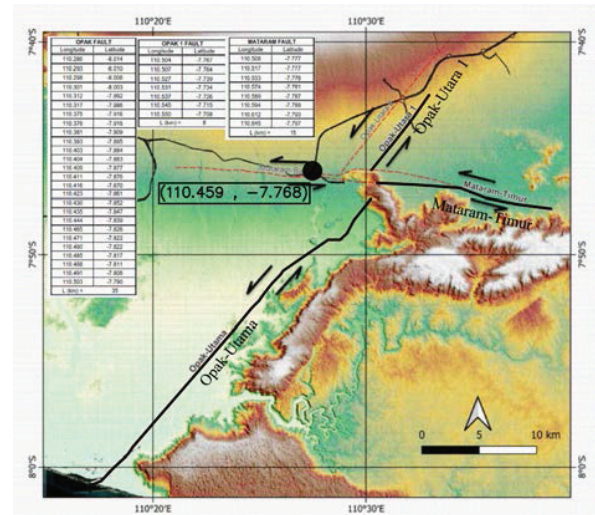


Fig. 1. Location of Three Shallow Crustal Faults.

DSHA was carried out by calculating the median (50%) response spectrum for three faults using three GMPEs with equal weights from NGA West2 (Pusgen, 2007) i.e. Boore & Atkinson (2013), Campbell & Bozorgnia (2013) and Chiou & Young (2013). The results are summarized in Fig. 2.

Tabel 1. Shallow Crustal Fault Characteristic

Fault Name	Slip rate (mm/yr)	Mechanism	M _{max}	Closest Distance
Opak Utama	2	Strike-slip	6.9	5.5
Opak 1	0.5	Strike-slip	6.1	5.1
Mataram Timur	2	Strike-slip	6.4	5.6

Fault Name	Dip (°)	Top (km)	Wide (km)	Long (km)
Opak Utama	50E	3	20	40
Opak 1	90	3	20	8
Mataram Timur	90	3	20	15

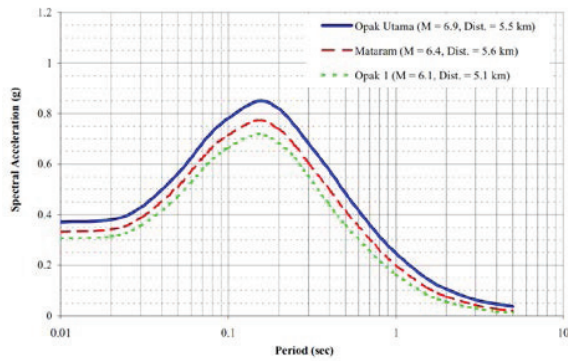


Fig. 2. Median rock spectrum based on DSHA

In order to obtain the response spectrum for 1000-year return period (RP), Probabilistic Seismic Hazard Analyses (PSHA) was also carried out by including all earthquake sources within 500 km radius from the project site. These sources contain subduction earthquakes (Megathrust & Benioff) and active shallow crustal faults ($M > 6.5$) and shallow background ($M < 6.5$). Using GMPE as specified by Pusgen (2007), response spectrum for RP 1000 years was developed; the results indicate the spectral acceleration (S_a) @ $T = 0, 0.2, 1$ and 2 seconds to be about 0.433 g , 0.990 g , 0.302 g and 0.142 g . Fig. 3 shows the Uniform Hazard Spectrum (UHS) for "bedrock" based on PSHA.

According to SNI 2833-2016, deterministic response spectrum shall be used for sites with known faults at distance less than 10 km and $M_w > 6$, as well as the median of deterministic response spectrum shall not be less than two-thirds ($2/3$) of the probabilistic response spectrum for RP-1000 years. Fig. 4 shows the median response spectrum from DSHA is controlling than the probabilistic ($2/3$ RP 1000 years) for $T = 0.5$ to $2 T_F$ where T_F is period of the bridge to be about 2 seconds.

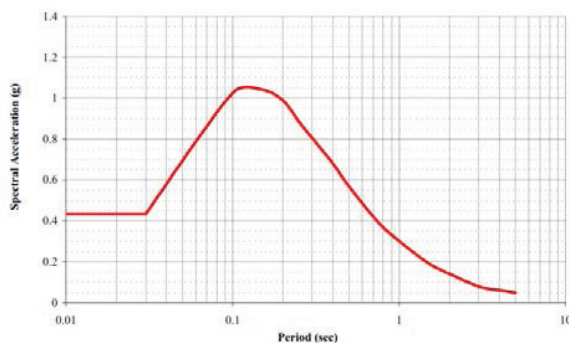


Fig. 3. Uniform Hazard Spectrum (UHS) for "Bedrock"

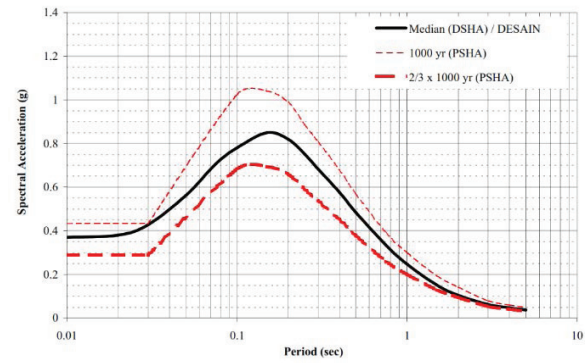


Fig. 4. Design Response Spectrum for "Bedrock"

3 RUPTURE DIRECTIVITY EFFECT

For sites that are close to the faults ($D < 10\text{ km}$, $M_w > 6$), the project can be classified as Near-Fault Sites (NFS). There are two factors that must be considered, namely the directivity and fling-step effects. Directivity can be classified as Forward or Backward directivity depending on the project site against wave propagation when rupture occurs (Fig. 5, Somerville, 2005). For this project, Opak Utama and Mataram faults can potentially cause forward directivity, due to two-sided velocity pulse in which result "constructive interference" from the same slip direction as fault start to rupture. Meanwhile, the "fling-step" effect only occurs due to the "one-sided velocity pulse" of tectonic deformation that occurs in the direction of the parallel fault for large earthquake magnitudes ($M_w > 7$, $D = 5\text{ km}$) as observed by Ancheta, 2016. Since the Mataram fault is located parallel to the location only up to $M_w 6.4$, the possibility of fling effect is small.

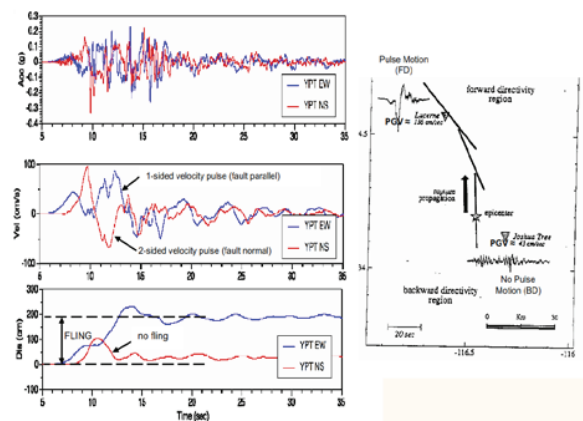


Fig. 5. Forward Directivity & Fling Effect

The effect of forward directivity and pulse motion is the occurrence of wave propagation in the normal fault direction (FN) which is

stronger than the direction of the fault parallel (FP). This has the potential to occur in the Main Opak fault. Therefore, the response spectrum shall be modified (adjusted) to account for the directivity effect, in form of an increase in spectral acceleration for $T > 0.75$ second. In order to calculate the effect of directivity, an empirical formula by Prof. Norman Abrahamson (2000) was used, the results indicate that for spectral acceleration of normal fault direction (FN), the value of S_a shall be increased by about 10% for $T > 0.75$ seconds (Fig. 6) as compared to fault parallel (FP).

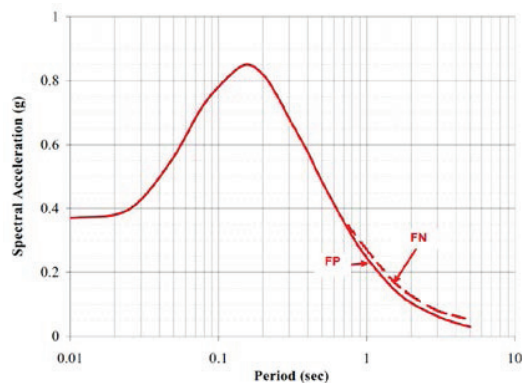


Fig. 6. FN & FP Response Spectrum

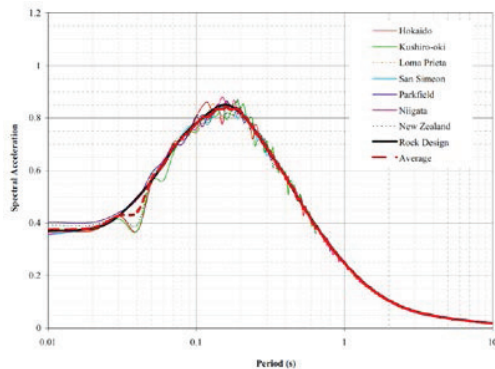


Fig. 7. Spectrally Matched Response Spectrum

Dynamic site response analyses were performed to propagate the earthquake shear wave from underlying bedrock ($V_s=760$ m/sec) to ground surface. It requires seven earthquake time series as "seed motion" to match the design response spectrum on rock. The time series were selected to represent different tectonic conditions of various types of earthquake sources such as subduction (Benioff & Megathrust) and active faults of

shallow earthquakes recorded on hard soils ($V_{s30}>400$ m/s) with the characteristics as listed on Table 2. These seed motions were spectrally-matched to design rock spectrum as shown on Fig. 7.

Tabel 2. Seed Motion Characteristic for bedrock

EQ Source	Event	Sta.	M_w	Depth (km)
Active Faults	2003 San Simeon	Temple-ton	6.5	9
	1996 Parkfield	Cholame	6.2	10
	1989 Loma Prieta	Anderson	6.9	18
	2004 Niigata	NGH12	6.6	11
	1987 NZ	Matahina	6.6	6
	1994 Hokkaido	47418	8.3	27
Mega-thrust	1993 Koshiro-oki	47409	7.6	107

4 DYNAMIC RESPONSE SPECTRUM

One-dimensional dynamic response analysis was performed to calculate the amplification of the response spectrum and peak ground acceleration (PGA) at the ground surface. The analysis was conducted using total-stress method (equivalent linear total stress) through computer software SHAKE.

Based on review of the existing soil borings, the subsurface contains medium dense to dense silty sand and stiff silt or sandy silt with water level at depths of 4.5 m. In addition, downhole seismic (DS) test was performed to depths of 30 m, where V_s comparison from DS test and empirical formula with N_{SPT} was consistent (Fig. 8A). For soil profiles below 30 m, it was assumed that V_s increases gradually (20 to 40 m/sec per 10 m depth) to bedrock level at depth of about 160 to 240 m (Fig. 8A). Shear modulus degradation and damping relationship with shear strain for sandy soils above 30 m using Seed-Idriss formula (1970) and for depths below 30 m using Darendeli formula (2001) as shown on Fig. 8B.

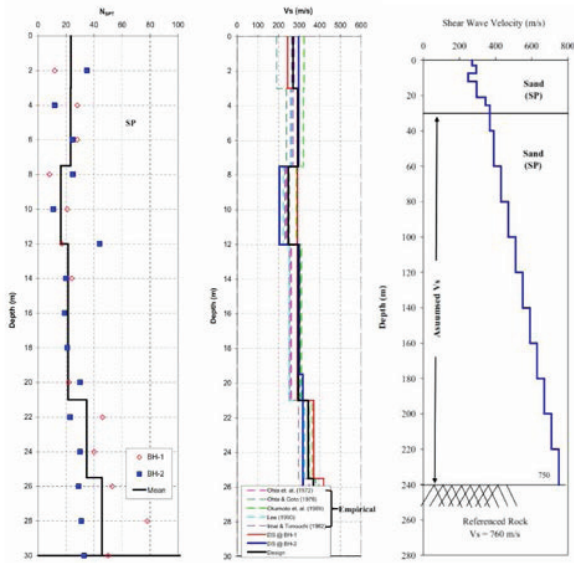


Fig. 8A. Vs Profile & Bedrock Assumption

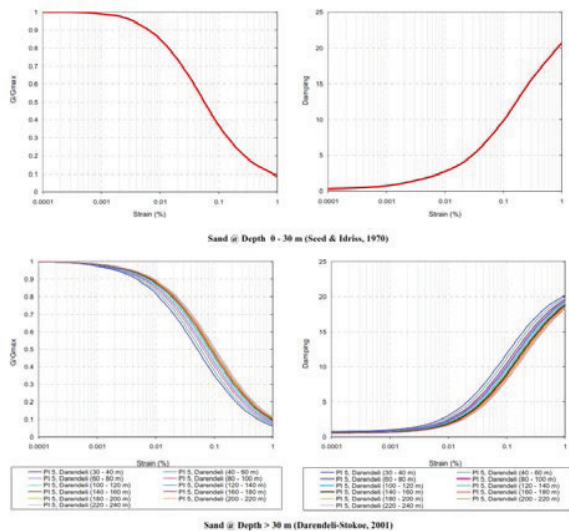


Fig. 8B. G/Gmax & Damping vs Strain

The results of dynamic response analysis are presented in form of amplification (the ratio of spectral acceleration on ground surface over spectral acceleration in rocks) as a function of the period, including the average values as shown in Fig. 9A for rock depths of 160, 200, and 240 m. In addition, comparison of soil amplification factors from GMPE using $V_{s30} = 300$ m / sec was carried out; the result is shown on Fig. 9B.

The design amplification was developed from the maximum envelop average value of SHAKE and GMPE. Fig. 10 shows that a) for peak ground acceleration ($T=0$ seconds), spectral acceleration increased (amplification) by 1.12, b) in low periods, S_{DS} ($T= 0.2$

seconds), spectral acceleration undergoes amplification by 1.04; and c) for a long period of S_{D1} ($T = 1$ second), the spectral acceleration undergoes amplification of 2.3. This amplification factor is consistent with the F_{PGA} , F_a and F_v of SNI-2833-2016 (for bridges) or SNI-1726-2019 (for buildings) as shown on Fig. 10.

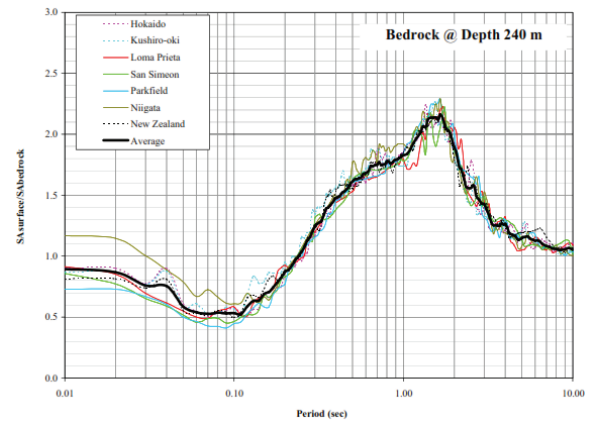


Fig. 9A. Amplification Factor at Ground Surface

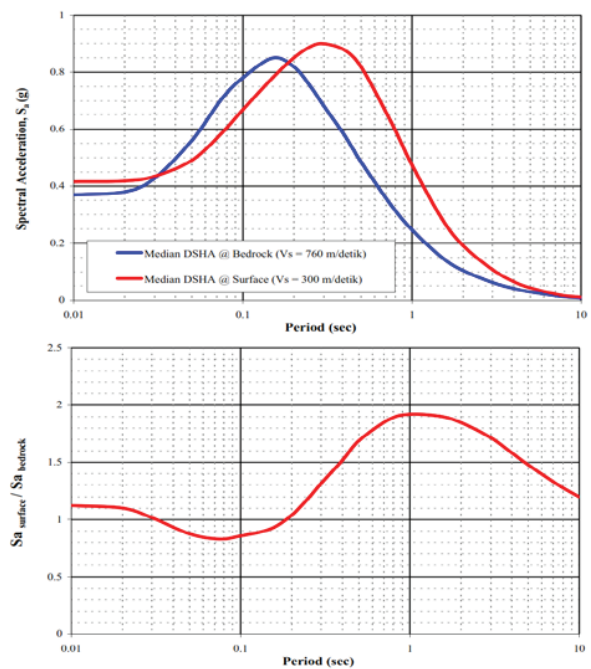


Fig. 9B. Amplification Factor from GMPE

The horizontal response spectrum at ground surface is taken from the multiplication between the amplification design (Fig. 10) and the rock spectrum (Fig. 6) in which the result is shown on Fig. 11. This design response spectrum envelops the result of SHAKE and GMPE analysis for $V_s = 300$ m/sec.

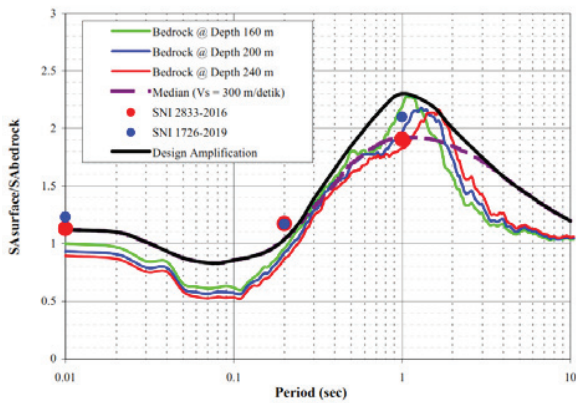


Fig. 10. Design Horizontal Amplification

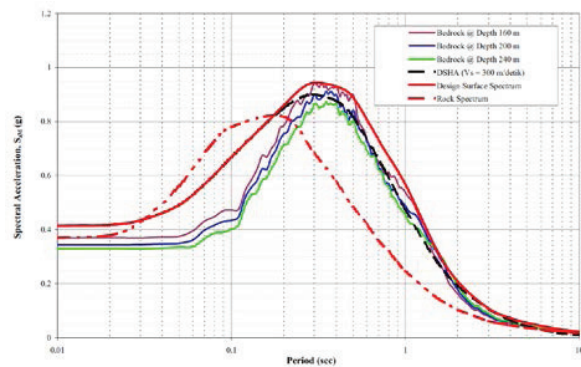


Fig. 11. Horizontal Response Spectrum

5 DESIGN HORIZONTAL & VERTICAL RESPONSE SPECTRUM

SNI 2833-2016 stipulates that spectral acceleration from site-specific response analyses (SSRA) shall not be smaller than two-thirds of the coded-spectrum for period of 0.5 to 2 T_F or $T=1$ to 4 second for $T_F=2$ seconds. Based on this requirement, adjustments were made to the response spectrum at ground surface by taking higher spectral acceleration for $T>3$ seconds to meet the coded spectrum (Fig. 12).

The vertical response spectrum is developed from multiplication of V/H factor by the horizontal response spectrum. The V/H factor is obtained from the vertical and horizontal GMPE formulations of Chiou & Young (2013) and Boore, et. al (2013) using M6.9, D5.5 km (Fig. 13). Fig. 14 shows the design response spectrum at ground surface in the horizontal and vertical directions, where the horizontal response spectrum is distinguished between normal fault (FN) and parallel fault (FP) due to NFS.

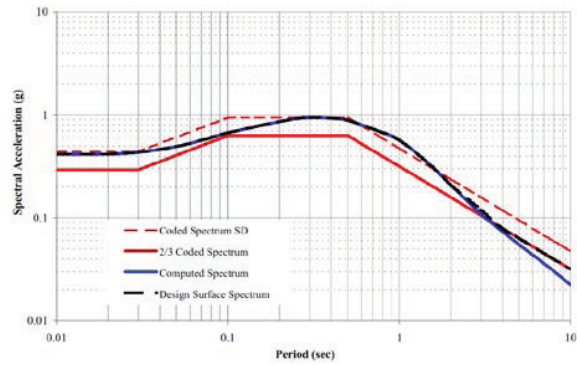


Fig. 12. Spectral Acceleration for $T>3$ second

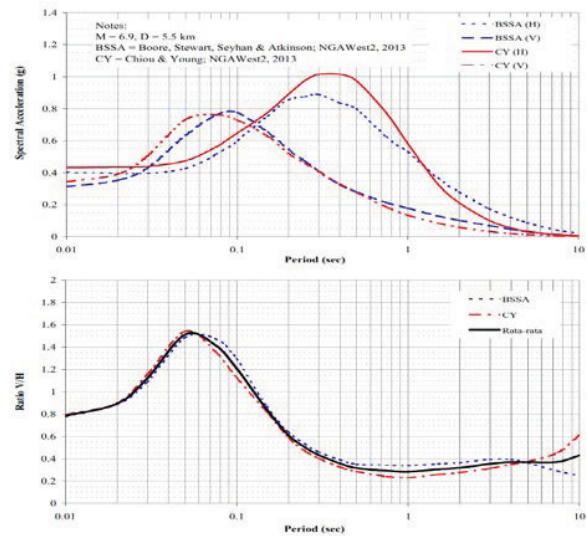


Fig. 13. V/H Factor Based on GMPE

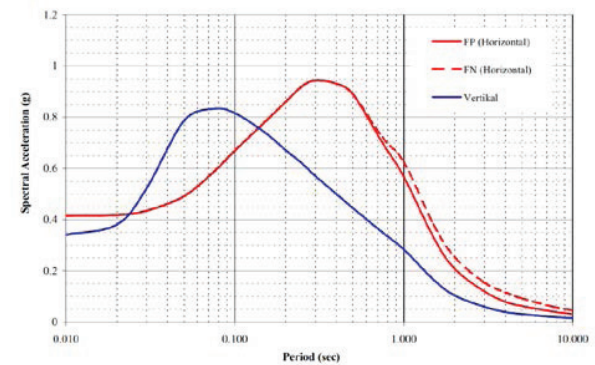


Fig. 14. Vertical & Horizontal Response Spectrum at Ground Surface

6 SELECTION OF TIME HISTORY AT GROUND SURFACE

Seven (7) sets of time series are required to match the surface response spectrum in the horizontal and vertical directions by considering the "pulse-motion" that occurs due to fault-normal (FN). According to Hayden & Bray (2014), for response spectrum with

epsilon = 0 (median) and fault distance of about 5 km, then 43% of the total (7) selected ground motion must be pulse motions (Fig. 15) with Peak Ground Velocity (PGV) ± 72 cm/sec (range 50-100 cm/sec) and pulse period (Tp) ± 1.7 seconds (range 1 to 2.5 seconds) following the empirical formula from Bray & Marek (2004) as follows:

$$\ln(\text{PGV}) = 4.46 + 0.34M_w - 0.58\ln(R^2 + 7^2) \pm \sigma_{\text{total}} \quad (1)$$

where $\sigma_{\text{total}} = 0.39$

$$\ln(\text{Tp}) = -5.6 + 1.32M_w \pm \sigma_{\text{total}} \quad (2)$$

where $\sigma_{\text{total}} = 0.58$

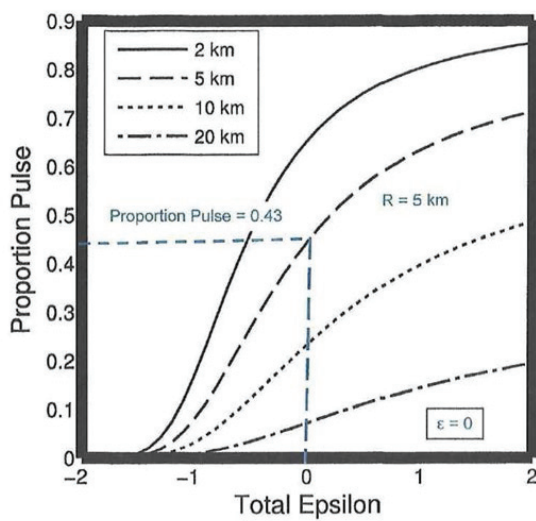


Fig 15. Pulse Motion Selection Criteria

This implies there will be (4) sets of no-pulse motions and (3) sets of pulse motions to represent the design earthquake (RP= 1000 years) as shown on Table 3.

For no-pulse motions, (2) sets from shallow crustal faults and (2) other sets from subduction source (Megathrust and Benioff) were scaled to the surface design spectrum in the FN and FP and vertical direction at period interest of 2 seconds. The average of (4) response spectra for no-pulse motions match the design spectra in the horizontal and vertical direction with scaling factors of about 1.26 to 4.23 as shown on Fig. 16. Duration of shaking for no pulse motions varies from about 15-25 sec (crustal) and 25-50 sec (subduction).

Criteria selection for pulse motion shall be the existence of distinct forward directivity pulses, similar faulting, magnitude and

distance to the site that correspond to desired pulse period and PGV where the maximum period of the velocity spectra meets the target structural period.

Three (3) sets time series were selected where FN direction should contain pulse motions with PGV and Tp close to the target PGV = 72 cm/s and Tp = 1.7 seconds. The selected motions were earthquake records from Northridge (PGV = 76 cm/s, Tp = 1.2 seconds), Irpinia earthquake (PGV = 72 cm/s, Tp = 3.3 seconds) and Loma Prieta (PGV = 43 cm/s, Tp = 1.6 seconds). PGV of the Loma Prieta record was scaled-up 1.6 times to reach the target PGV = 72 cm/s. For pulse motions, velocity response spectrum is more critical than the acceleration response spectrum. The average of three velocity spectra from pulse motions in the horizontal (FN & FP) is presented on Fig. 17. The maximum velocity spectral acceleration reaches the maximum values at T=1.2 to 3 seconds, approaching the period T_F of the bridge structure (= 2 seconds). Duration of shaking for typical pulse motions are typically short (less than 10 second).

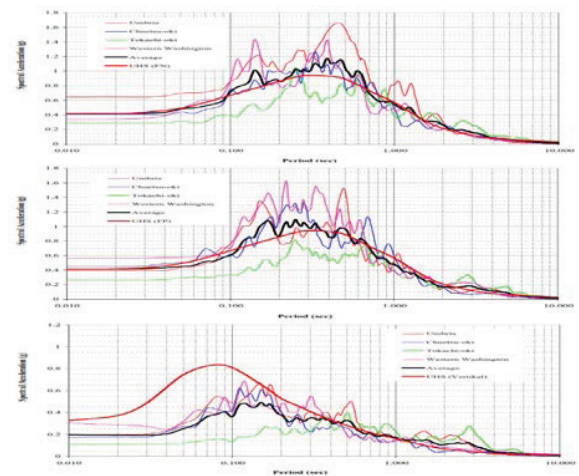


Fig 16. Spectral Acceleration for (4) No-Pulse Motions

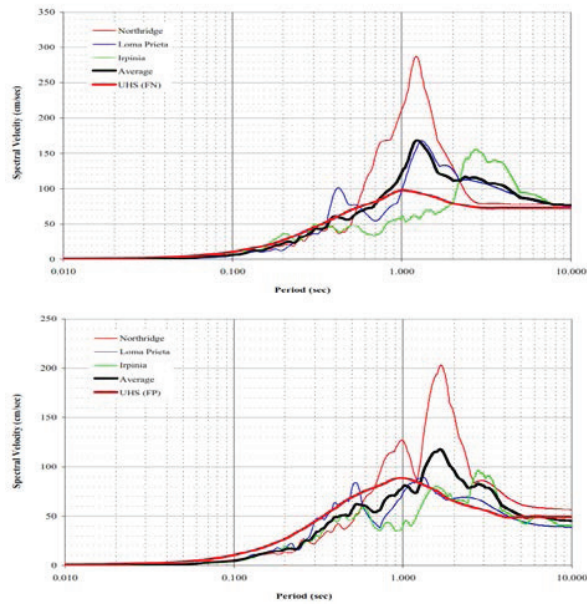


Fig 17. Velocity Spectral Acceleration for (3) Pulse Motions

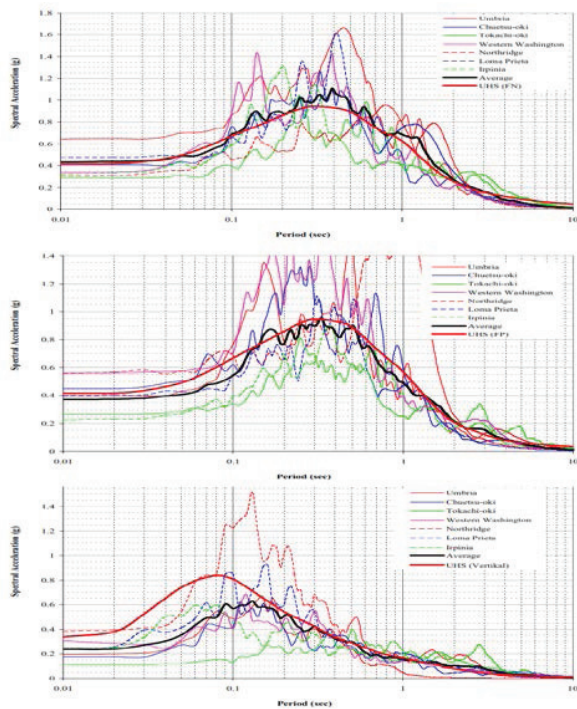


Fig 18. Spectral Acceleration for All (7) Motions

Table 3. Characteristic of (7) sets of Time Series

Event	RSN	M _w	Depth (km)	Distance (km)	Scale Factor
1997 Umbria Marche, Italy	4348	6	6	17	3.73
2007 Chuetsu- oki, Japan	4866	6.8	9	12	1.26
1994 North- ridge, CA	1054	6.7	31	6	1.00
1989 Loma Prieta, CA	764	6.9	33	10	1.60
1980 Irpinia, Italy	292	6.9	33	7	1.00
Tokachi- oki	40284 38	8.4	32	188	4.23
Western Washing- ton	Olym- pia	6.9	70	75	2.06

7 NLTHA FOR BRIDGES

According to SNI 2833-2016, the time series in the normal fault direction (FN) and parallel faults (FP) of the mapped fault should be used simultaneously and rotated to the transverse and longitudinal components of the bridge structure.

Non-Linear Time History Analysis (NLTHA) was applied on Jogja-Solo Toll Road Section 2.1 Project. As seen in the Fig. 19, site plan of the toll road is located perpendicular to the Opak Fault, such that time series in fault-normal (FN) is applied to long direction of the bridge. While fault parallel (FP) is applied to transverse direction of the viaduct.



Fig 19. Site Plan Toll Road and Opak Fault

Structural viaducts use PC-U girders of 45 m with the span length 47 m (Fig. 20) and used Lead Rubber Bearing (LRB) for the bearings. Bridge modelling is shown on Fig. 21 using Midas Civil version 19.1.

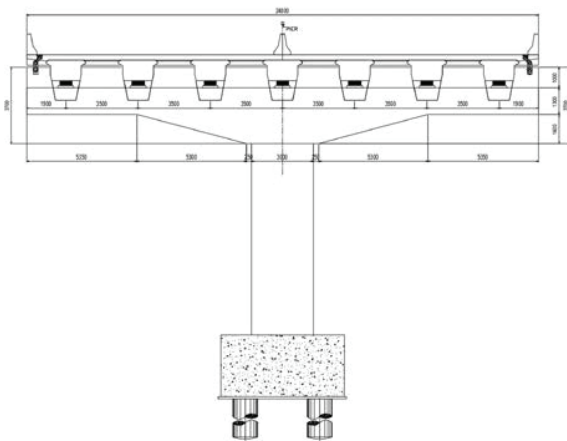


Fig 20. Cross Section of the structure

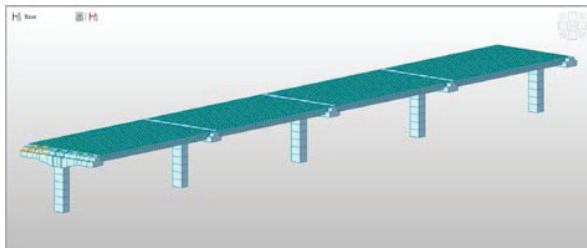


Fig 21. 3D Modeling

The modeling result is shown as Table 4, where time period (mode-1) is 2.776s in Y-translation and 2.77s in mode-2 in X-translation.

Table 4. Time Period and Modal Participation Mass

Mod No	Period (sec)	Tran-X		Tran-Y	
		Mass (%)	Sum (%)	Mass (%)	Sum (%)
1	2.776996	0	0	24.78	24.78
2	2.770365	41.76	41.76	0	24.78

Mod No	Period (sec)	Tran-Z		ROTN-X	
		Mass (%)	Sum (%)	Mass (%)	Sum (%)
1	2.776996	0	0	0	0
2	2.770365	0	0	0	0

Mod No	Period (sec)	ROTN-Y		ROTN-Z	
		Mass (%)	Sum (%)	Mass (%)	Sum (%)
1	2.776996	0	0	0	0
2	2.770365	1.63	1.63	0	0

The results of average LRB movement for seven time series are shown in Fig. 22, where the maximum average movement is 100 mm, while LRB movement capacity is 215 mm.

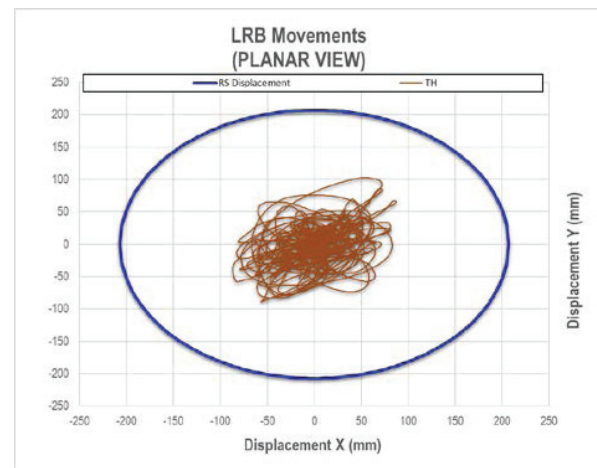


Fig 22. LRB Movement Average Result

8 CONCLUSION

The effect of forward directivity will cause "pulse motion" such that the response spectrum must be distinguished between normal faults (FN) and parallel faults (FP) for a period of > 0.75 seconds. The selection of time history in the fault normal (FN) should take into account the presence of "pulse motion".

Selection of seven sets time series shall include four set time series for no-pulse motions taken from crustal faults and subduction earthquakes as well as three other sets for "pulse motions" taken from near-fault earthquake catalogs that have $PGV = 72$ cm / sec and $Tp = 1.7$ seconds.

Selection of time series was carried out using "direct scaling" method against the seed motions with scale factors of 1.26 to 4.23. The average response spectrum of the scaled motion well-match to the horizontal design spectrum in the FN and FP direction at T=1 to 4 seconds and vertical design spectrum at period of 0.6 to 2 seconds (Fig. 18). The peak velocity spectrum of pulse motions, particularly in the FN direction, is at T=1.2 to 3 seconds, close to the period of interest of the bridge. The duration of the earthquake also varies from short duration of 10 seconds (NFS) and long duration of 50 seconds (Megathrust).

9 ACKNOWLEDGMENTS

We express our gratitude and appreciation to Mr. Tutus Trihandoko as the Technical General Manager of PT Jogjasolo Marga Makmur (JMM) that allowing us to publish part of this study report. The first author thanks to Dr. Ezra YS Tjung of Calvin Institute of Technology (Jakarta) to proof-read this manuscript.

REFERENCE

- AASHTO (2012): "*LRFD Bridge Design Specification*".
- Abrahamson, N. A. (2000), "*Effects of rupture directivity on probabilistic seismic hazard analyses*", Proceeding, 6th International Conference on Seismic Zonation, EERI, Oakland CA.
- Ancheta, T.D. (2016), "*Empirical Data with Fling Effect*". Presentation during PEER workshop, Berkeley.
- Alavi, B. and Krawinkler, H. (2004), "*Behavior of moment-resisting frame structures subjected to near-fault ground motions*", Earthquake Engineering & Structural Dynamics 33(6) 687-706.
- Badan Standardisasi Nasional (2016): "*SNI 2833:2016 Perencanaan Jembatan Terhadap Beban Gempa*".
- Bray, J.D. and Marek, A. (2004), "*Characterization of forward-directivity ground motions in the near-fault region*" Soil Dynamics and Earthquake Engineering · December 2004.
- Hayden, C., Bray, J. and Abrahamson, N.A. (2014), "*Selection of Near-field Pulse Motions*" Journal of Geotechnical and Environmental Engineering, ASCE, Vol. 140 (7), 04014030
- M.B. Darendeli, (2001): "*Development of a New Family of Normalized Modulus Reduction and Material Damping Curves*", Ph.D thesis, under Professor Dr. K.H. Stokoe at the University of Texas at Austin.
- PEER (2013), "*NGA-West2 Ground Motion Prediction Equations for Vertical Ground Motions*" report. No. 2013-24.
- Pusat Studi Gempa Nasional, Pusat Litbang Perumahan dan Pemukiman/ PUSGEN (2017): "*Peta Sumber dan Bahaya Gempa Indonesia tahun 2017*".
- Somerville, P.G. (2005), "*Engineering characterization of near-fault ground motion*", NZSEE Conference.